Wang, Olevsky, et al. Published in Mechanics Research Communications 33. 2006: 53-62.

# Stability analysis for forging of porous bodies

Xuan Wang [a], Eugene Olevsky [a,*], Alain Molinari [b]

[a] San Diego State University, Mechanical Engineering Department, 5500 Campanile Drive, San Diego, CA 92182-1323, USA
[b] Laboratoire de physique et mécanique des matériaux, ISGMP, ENIM, Université de Metz, Ile du Saulcy, 57045 Metz Cedex 1, France

**Abstract**

The continuum theory of sintering is used for the analysis of the stability of forging of a cylindrical powder specimen. The constitutive properties of the powder material are assumed to follow a power-law creep relationship. Temperature-coupled linear non-uniform stability analyses are carried out. Stability maps are obtained for forging of copper powder components.

*Keywords:* Powder; Porous materials; Forging; Continuum modeling; Stability analysis

## 1. Introduction

Macroscopic deformation of porous and powder materials have been considered by various researchers during the last two decades. Among the successful approaches in this area, continuum theories of sintering should be mentioned. Recently, along with the refinement and the creation of new constitutive models, the research focus was on the solution of certain boundary-value problems associated with industrial treatment of porous and powder products.

For hot deformation processes, as experimental practice indicates, the dominant mechanism is the power-law creep (see Ashby, 1990; Wilkinson and Ashby, 1975) which is usually described by Ashby relationship

$$\frac{\sigma}{\sigma_0} = A\left(\frac{\dot{\varepsilon}}{\dot{\varepsilon}_0}\right)^m \tag{1}$$

where $\sigma$ and $\dot{\varepsilon}$ are the stress and strain rate, respectively; $A$, $\sigma_0$, $\dot{\varepsilon}_0$, and $m$ are material parameters.

* Corresponding author. Tel.: +1 619 594 6329; fax: +1 619 594 3599.
*E-mail address:* olevsky@kahuna.sdsu.edu (E. Olevsky).

**Nomenclature**

| | |
|---|---|
| $A$ | pre-exponential factor in the power-law creep relationship |
| $c$ | heat capacity of the porous material |
| $\dot{e}$ | volume change rate (first invariant of the strain rate tensor) |
| $F_z$ | constant axial externally applied force |
| $h$ | sample current height |
| $h_0$ | sample initial height |
| $m$ | strain rate sensitivity |
| $n$ | loading mode parameter |
| $p$ | hydrostatic stress |
| $Q_c$ | activation energy in the power-law creep relationship |
| $R$ | sample current radius |
| $R_g$ | gas constant |
| $S$ | cross-sectional area of the porous specimen |
| $S_i$ | initial cross-sectional area of the porous specimen |
| $T$ | absolute temperature |
| $t$ | time |
| $W$ | equivalent strain rate |
| $\delta_{ij}$ | Kronecker's symbol |
| $\dot{\varepsilon}_{ij}$ | components of the strain rate tensor |
| $\dot{\varepsilon}_1, \dot{\varepsilon}_2, \dot{\varepsilon}_3$ | main elongation rates |
| $\dot{\varepsilon}_0$ | reference strain rate |
| $\dot{\varepsilon}_r, \dot{\varepsilon}_z$ | radial and axial strain rates |
| $\dot{\gamma}$ | shape change rate (second invariant of the strain rate tensor deviator) |
| $\eta_0$ | shear viscosity of the sample's skeleton material |
| $\lambda$ | perturbation growth rate |
| $\theta$ | sample porosity |
| $\varphi$ | porous material normalized shear viscosity modulus |
| $\psi$ | porous material normalized bulk viscosity modulus |
| $\theta_i$ | sample initial porosity |
| $\rho$ | density of the porous material |
| $\sigma_0$ | reference stress |
| $\sigma_{ij}$ | components of the stress tensor |
| $\sigma_z$ | axial stress component |
| $\sigma(W)$ | equivalent stress |
| $\tau$ | second invariant of the deviatoric stress |
| $\tau_0$ | yield limit of a full-dense material |
| $\tau_F$ | the dimensionless time of loading |
| $\upsilon$ | constant cross-head velocity |

Stability of material flow and localization phenomena are very important aspects of powder processing. The analysis of the stability of the deformation of porous and powder materials is a new area represented in a very limited number of publications, for example, the publications of Zhang and Lee (see Lee and Zhang, 1994, 1996), which are limited to the analysis of cold forging.

This study is a logical continuation of the previous work of Olevsky and Molinari (see Olevsky and Molinari, 2000). Forging deformation process is considered here. The material behavior is assumed to obey a power-law creep, and strain hardening is neglected. The continuum theory of sintering (see Olevsky et al., 1996, 1997; Olevsky, 1998; Olevsky and German, 2000a,b; Olevsky and Molinari, 2000) is used as a basis for the present work.

## 2. Constitutive behavior of viscous porous bodies

### 2.1. Basic constitutive equations of nonlinear viscous porous bodies

The mechanical response of a porous body with power-law creep behavior is described by a rheological (constitutive) relation that inter-relates the components of a stress tensor $\sigma_{ij}$ and a strain rate tensor $\dot{\varepsilon}_{ij}$ (see Olevsky and Molinari, 2000):

$$\sigma_{ij} = \frac{\sigma(W)}{W}\left[\varphi\dot{\varepsilon}_{ij} + \left(\psi - \frac{1}{3}\varphi\right)\dot{e}\delta_{ij}\right] \tag{2}$$

where $\varphi$ and $\psi$ are the normalized shear and bulk viscosity moduli, which depend on porosity $\theta$ (for example, following Skorohod (see also Table 1), $\varphi = (1-\theta)^2$, $\psi = \frac{2}{3}\frac{(1-\theta)^3}{\theta}$); $\delta_{ij}$ is a Kronecker symbol ($\delta_{ij} = 1$ if $i = j$ and $\delta_{ij} = 0$ if $i \neq j$); $\dot{e}$ is the first invariant of the strain rate tensor, i.e. sum of tensor diagonal components: $\dot{e} = \dot{\varepsilon}_{11} + \dot{\varepsilon}_{22} + \dot{\varepsilon}_{33}$. Physically, $\dot{e}$ represents the local volume change rate of a porous body.

The porosity $\theta$ is defined as $1 - \frac{\rho}{\rho_T}$, where $\rho$ and $\rho_T$ are volumetric mass and theoretical density (volumetric mass of a fully dense material), respectively.

The effective equivalent strain rate $W$ is connected with the current porosity and with the invariants of the strain rate tensor

$$W = \frac{1}{\sqrt{1-\theta}}\sqrt{\varphi\dot{\gamma}^2 + \psi\dot{e}^2} \tag{3}$$

where $\dot{\gamma}$ is the second invariant of the strain rate tensor deviator

$$\dot{\gamma} = \left[\left(\dot{\varepsilon}_{ij} - \frac{1}{3}\dot{e}\delta_{ij}\right)\left(\dot{\varepsilon}_{ij} - \frac{1}{3}\dot{e}\delta_{ij}\right)\right]^{1/2} \tag{4}$$

Physically, $\dot{\gamma}$ represents the shape change rate of a porous body.

The energy conservation equation can be written as

$$\rho c\dot{T} = \frac{\sigma(w)}{w}(\varphi\dot{\gamma}^2 + \psi\dot{e}^2) \tag{5}$$

Table 1
Normalized shear and bulk moduli for four different models

| Model/Parameter | $\varphi$ | $\psi$ |
|---|---|---|
| Skorohod | $(1-\theta)^2$ | $\frac{2}{3}\frac{(1-\theta)^3}{\theta}$ |
| Castaneda–Duva–Crow | $\frac{(1-\theta)^{\frac{2}{1+m}}}{1+\frac{2}{5}\theta}$ | $\frac{2}{3}\left(\frac{1-\theta^m}{m\theta^m}\right)^{\frac{2}{m+1}}$ |
| McMeeking-Sofronis | $\left(\frac{1-\theta}{1+\theta}\right)^{\frac{2}{1+m}}$ | $\frac{2}{3}\left(\frac{1-\theta^m}{m\theta^m}\right)^{\frac{2}{m+1}}$ |
| Cocks | $\frac{(1-\theta)^{\frac{2}{1+m}}}{1+\frac{2}{5}\theta}$ | $\frac{m+1}{3}\frac{(1+\theta)(1-\theta)^{\frac{2}{m+1}}}{\theta}$ |

where $\rho$ is density, $c$ is heat capacity (both $\rho$ and $c$ are functions of porosity $\theta$) and $\dot{T}$ is the time derivative of temperature $T$. Heat conduction effects have been neglected in (5).

Let us consider a loading process where the stress tensor has the form

$$[\sigma_{ij}] = \begin{pmatrix} \sigma_r & 0 & 0 \\ 0 & \sigma_r & 0 \\ 0 & 0 & \sigma_z \end{pmatrix} \tag{6}$$

$\sigma_z$ and $\sigma_r$ are the axial and the radial stresses, respectively.

In this case, the two first stress invariants can be represented as

$$p = \frac{\sigma_{ii}}{3}; \quad \tau = ((\sigma_{ij} - p\delta_{ij})(\sigma_{ij} - p\delta_{ij}))^{1/2} \tag{7}$$

When a lateral confinement of the powder specimen is present or isostatic pressing is employed, one can introduce a loading mode parameter $n$:

$$n = \frac{\tau}{p} \tag{8}$$

In the following analysis, loading modes with constant values of $n$ are considered.

The ratio between the rate of shape change and the rate of volume change is

$$\frac{\dot{\gamma}}{\dot{e}} = \frac{\psi}{\varphi}\frac{\tau}{p} = \frac{\psi}{\varphi}n \tag{9}$$

Hence, the equivalent strain rate assumes the form

$$W = \frac{|\dot{e}|}{\sqrt{1-\theta}}\sqrt{\psi}\sqrt{\frac{\varphi}{\psi}n^2 + 1} \tag{10}$$

### 2.2. Application to axisymmetric porous bodies

Let us consider a particular geometry with rotational symmetry with respect to the axis $z$ (see Fig. 1). If $\dot{\varepsilon}_z$ and $\dot{\varepsilon}_r$ are the axial and radial strain rates respectively then

$$\dot{e} = \dot{\varepsilon}_z + 2\dot{\varepsilon}_r; \quad \dot{\gamma} = \sqrt{\frac{2}{3}}|\dot{\varepsilon}_z - \dot{\varepsilon}_r| \tag{11}$$

Eq. (7) can be reduced to

$$p = \frac{1}{3}(\sigma_z + 2\sigma_r); \quad \tau = \sqrt{\frac{2}{3}}|\sigma_z - \sigma_r| \tag{12}$$

From Eqs. (7), (11) and (12) one can obtain

$$\sigma_z = \frac{\sigma(w)}{w}\psi\dot{e}\left[\sqrt{\frac{2}{3}}\mathrm{sgn}(\sigma_z)n + 1\right] \tag{13}$$

The evolution law of porosity is given by

$$\dot{e} = \frac{\dot{\theta}}{1-\theta} \tag{14}$$

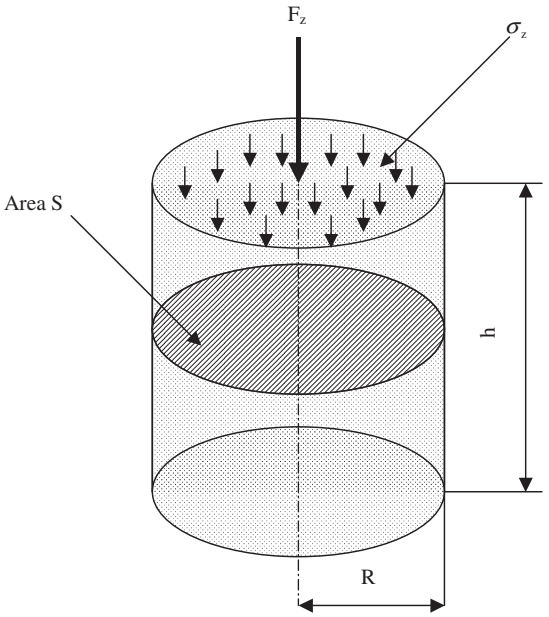


Fig. 1. Cylindrical porous specimen.

### 2.3. Kinetics of porosity and evolution of the cross-section area

In view of (1), (3), (13) and (14), the following kinetic expression is valid:

$$\dot{\theta} = \mathrm{sgn}(p)\left[\frac{|\sigma_z|}{A\sigma_0}\right]^{\frac{1}{m}} \dot{\varepsilon}_0(1-\theta)\left[\frac{1}{\psi\left|\sqrt{\frac{2}{3}}\mathrm{sgn}(\sigma_z)n+1\right|}\right]^{\frac{1}{m}}\left[\frac{\psi\left(\frac{\psi}{\varphi}n^2+1\right)}{1-\theta}\right]^{\frac{1-m}{2m}} \tag{15}$$

The cross-section area of the element is given by

$$S = \pi R^2 \tag{16}$$

It can be shown that (see Olevsky and Molinari, 2000):

$$\frac{\mathrm{d}[\ln S]}{\mathrm{d}\theta} = 2\frac{\frac{\varphi}{3}-\frac{\psi}{\sqrt{6}}|n|}{\varphi(1-\theta)} \tag{17}$$

## 3. Temperature-coupled stability analysis

A spatial non-uniformity perturbation can be introduced in the form ($i$ is the imaginary unit):

$$Y(z,t) = Y^{(0)}(t) + \delta Y^{(0)}\exp(\lambda(t-t_0))\exp(\mathrm{i}\xi z) \tag{18}$$

where $Y$ represents the stress, porosity, or shrinkage rate. $\delta Y^{(0)}$ characterizes the amplitude of the perturbation, $\xi$ is the wave number, $t$ is time, and $t_0$ is the instant when the perturbation is introduced. The real part of $\lambda$ is the perturbation growth rate. If, for $t = t_0$, $\mathrm{Re}(\lambda) > 0$, the perturbation grows and the problem is said to be linearly unstable.

One can obtain from Eqs. (1), (5), (11) and (13)

$$\rho c\dot{T} = \frac{\sigma_z\left[\frac{\psi}{\varphi}n^2+1\right]}{\sqrt{\frac{2}{3}}\mathrm{sgn}(\sigma_z)n+1}\frac{\dot{\theta}}{(1-\theta)^2} \tag{19}$$

The relationship between stress and applied force is

$$F_z = \sigma_z S \tag{20}$$

In order to analyze the linear non-uniform temperature-coupled case, Eqs. (15), (17), (19) and (20) should be perturbed with respect to $\delta T$, $\delta\theta$, $\delta\sigma_z$, $\delta S$.

Eq. (19) can be written as (assuming that $\rho = \rho_0(1-\theta)$, $c = c_0(1-\theta)$):

$$\rho_0 c_0 \dot{T} = \sigma_z \varpi(\theta)\dot{\theta} \tag{21}$$

where

$$\varpi(\theta) = \frac{\left(\frac{\psi}{\varphi}n^2+1\right)}{\sqrt{\frac{2}{3}}\mathrm{sgn}(\sigma_z)n+1}\frac{1}{(1-\theta)^4} \tag{22}$$

Perturbing (21), one obtains

$$\rho_0 c_0 \frac{\lambda}{\dot{\theta}}\delta T - \sigma_z\left[\varpi' + \frac{\lambda}{\dot{\theta}}\varpi\right]\delta\theta - \varpi\delta\sigma_z = 0 \tag{23}$$

Eq. (15) can be expressed as

$$A^{\frac{1}{m}}\dot{\theta} = |\sigma_z|^{\frac{1}{m}}\Omega(\theta) \tag{24}$$

where

$$\Omega(\theta) = \mathrm{sgn}(\sigma_z)\dot{\varepsilon}_0(1-\theta)\left[\frac{1}{\sigma_0\psi\left|\sqrt{\frac{2}{3}}\mathrm{sgn}(\sigma_z)n+1\right|}\right]^{\frac{1}{m}}\left[\frac{\psi\left(\frac{\psi}{\varphi}n^2+1\right)}{1-\theta}\right]^{\frac{1-m}{2m}} \tag{25}$$

The material constant $A$ in Eq. (24) is a temperature dependent function

$$A = A_0\exp\left(\frac{A_1}{T}+A_2\right) \tag{26}$$

where $A_0$, $A_1$, and $A_2$ are material constants, and

$$A_1 = \frac{Q_c}{R_g} \tag{27}$$

where $Q_c$ is a creep activation energy, $R_g$ is the gas constant.

Eq. (26) can be rewritten in terms of the normalized temperature $\overline{T}$, and in terms of the initial temperature $T_i$

$$A = A_0\exp\left(\frac{Q_c}{R_g T_i\overline{T}}+A_2\right) \tag{28}$$

Perturbing (24), we have

$$\frac{A'_T}{mA}\delta T + \left(\frac{\lambda}{\dot{\theta}}-\frac{\Omega'}{\Omega}\right)\delta\theta - \frac{1}{m\sigma_z}\delta\sigma_z = 0 \tag{29}$$

where

$$\Omega' = \frac{\mathrm{d}\Omega}{\mathrm{d}\theta}$$

After perturbing Eqs. (17) and (20) the results can be expressed as follows:

$$\begin{bmatrix} \rho_0 c_0 \frac{\lambda}{\varpi\dot{\theta}} & -\sigma_z\left(\frac{\varpi'}{\varpi}+\frac{\dot{\lambda}}{\dot{\theta}}\right) & -1 & 0 \\ \frac{A'_{\mathrm{T}}}{A} & \frac{m\lambda}{\dot{\theta}} - \frac{m\Omega'}{\Omega} & -\frac{1}{\sigma_z} & 0 \\ 0 & 0 & S & \sigma_z \\ 0 & -\left(\frac{\dot{\lambda}}{\dot{\theta}}+\frac{\hat{G}'_\theta}{\hat{G}_\theta}\right) & 0 & \frac{1}{S}\left(\frac{1}{\hat{G}_\theta}\frac{\dot{\lambda}}{\dot{\theta}}-1\right) \end{bmatrix} \begin{bmatrix} \delta T \\ \delta\theta \\ \delta\sigma_z \\ \delta S \end{bmatrix} = 0 \tag{30}$$

where

$$\hat{G} = 2\frac{\frac{\varphi}{3}-\frac{\psi}{\sqrt{6}}|n|}{\varphi(1-\theta)}; \quad \hat{G}'_\theta = \frac{\mathrm{d}\hat{G}}{\mathrm{d}\theta} \tag{31}$$

and

$$A'_{\mathrm{T}} = \frac{\mathrm{d}A}{\mathrm{d}T} = -A\frac{Q_{\mathrm{c}}}{R_{\mathrm{g}}(T)^2} \tag{32}$$

By substituting (22), (25), (31) and (32) into (30) the following equation can be derived:

$$\begin{bmatrix} \rho_0 c_0 \frac{\dot{\lambda}}{\dot{\theta}} \frac{\left[\sqrt{\frac{2}{3}}\mathrm{sgn}(\sigma_z)n+1\right](1-\theta)^4}{\left(\frac{\psi}{\varphi}n^2+1\right)} & -\sigma_z\left[\frac{4}{1-\theta}+\frac{\varphi\psi' n^2-\psi\varphi' n^2}{\varphi\psi n^2+\varphi^2}+\frac{\dot{\lambda}}{\dot{\theta}}\right] & -1 & 0 \\ -\frac{Q_{\mathrm{c}}}{R_{\mathrm{g}}T^2} & \frac{m\lambda}{\dot{\theta}} - \frac{1}{2}n^2\left(\psi' - \frac{\psi\varphi'}{\varphi}\right)\cdot\frac{1-m}{\varphi\left(\frac{\psi}{\varphi}n^2+1\right)} - \frac{1-3m}{2(1-\theta)} + \frac{\psi'(1+m)}{2\psi} & -\frac{1}{\sigma_z} & 0 \\ 0 & 0 & S & \sigma_z \\ 0 & -\left(\frac{\dot{\lambda}}{\dot{\theta}}+\frac{(1-\theta)(\varphi\psi'-\varphi'\psi)-\sqrt{\frac{2}{3}}\frac{\varphi^2}{|n|}+\varphi\psi}{\varphi(1-\theta)(\psi-\sqrt{\frac{2}{3}}\frac{\varphi}{|n|})}\right) & 0 & \frac{1}{S}\left(\frac{\varphi(1-\theta)}{\left(\frac{2\varphi}{3}-\sqrt{\frac{2}{3}}\psi|n|\right)}\cdot\frac{\dot{\lambda}}{\dot{\theta}}-1\right) \end{bmatrix} \begin{bmatrix} \delta T \\ \delta\theta \\ \delta\sigma_z \\ \delta S \end{bmatrix} = 0 \tag{33}$$

If Eq. (33) has non-trivial solution, the determinant of the matrix in (33) should be equal to zero. Thus, we have

$$\left(\frac{\lambda}{\dot{\theta}}\right)^3 + D_1\left(\frac{\lambda}{\dot{\theta}}\right)^2 + D_2\left(\frac{\lambda}{\dot{\theta}}\right) + D_3 = 0 \tag{34}$$

where

$$\begin{aligned} D_1 = {} & \frac{2\phi}{3m} - \frac{\sqrt{6}|n|\psi}{3m} + \frac{\psi A'_{\mathrm{T}}\sigma_z n^2}{(1-\theta)^4 A\rho_0 c_0 m\phi\left(\frac{\sqrt{6}}{3}\mathrm{sgn}(\sigma_z)n+1\right)} + \frac{A'_{\mathrm{T}}\sigma_z}{(1-\theta)^4 A\rho_0 c_0 m\left(\frac{\sqrt{6}}{3}\mathrm{sgn}(\sigma_z)n+1\right)} - \frac{2\phi}{3} \\ & + \frac{\sqrt{6}}{3}\psi|n| - \frac{\psi' n^2}{2\left(\frac{\psi}{\phi}n^2+1\right)m\phi} + \frac{\psi n^2\phi'}{2\left(\frac{\psi}{\phi}n^2+1\right)m\phi^2} + \frac{\psi' n^2}{2\left(\frac{\psi}{\phi}n^2+1\right)\phi} - \frac{\psi n^2\phi'}{22\left(\frac{\psi}{\phi}n^2+1\right)\phi^2} \\ & + \frac{3}{2(1-\theta)} - \frac{1}{2m(1-\theta)} + \frac{\psi'}{2\psi} + \frac{\psi'}{2\psi m} \end{aligned}$$

$$D_2 = \left(\frac{\psi}{\phi}n^2 + 1\right)\frac{\frac{2\phi}{3} - \frac{\sqrt{6}}{3}\psi|n|}{A\rho_0 c_0(\frac{\sqrt{6}}{3}\,\mathrm{sgn}(\sigma_z)n + 1)}\left\{\rho_0 c_0\left(\frac{\sqrt{6}}{3}\,\mathrm{sgn}(\sigma_z)n + 1\right)(1-\theta)^3\right.$$

$$\times A\frac{(1-\theta)(\phi\psi' - \psi\phi') - \frac{\sqrt{6}\phi^2}{3|n|} + \phi\psi}{\phi\left(\frac{\psi}{\phi}n^2 + 1\right)\left(\psi - \frac{\sqrt{6}\phi}{3|n|}\right)} - 2A'_{\mathrm{T}}\sigma_z + A'_{\mathrm{T}}\sigma_z\left(\frac{4}{1-\theta} + \frac{\phi\psi' n^2 - \psi\phi' n^2}{\phi\psi n^2 + \phi^2}\right)\frac{\phi(1-\theta)}{\frac{2}{3}\phi - \frac{\sqrt{6}}{3}\psi|n|}$$

$$\left. - \frac{A\rho_0 c_0}{\left(\frac{\psi}{\phi}n^2 + 1\right)}\left(\frac{\sqrt{6}}{3}\,\mathrm{sgn}(\sigma_z)n + 1\right)(1-\theta)^4\left[-\frac{1-3m}{2(1-\theta)} - \frac{n^2(\psi' - \frac{\psi\phi'}{\phi})(1-m)}{2\phi\left(\frac{\psi}{\phi}n^2 + 1\right)} + \frac{\psi'(1+m)}{2\psi}\right]\right\}$$

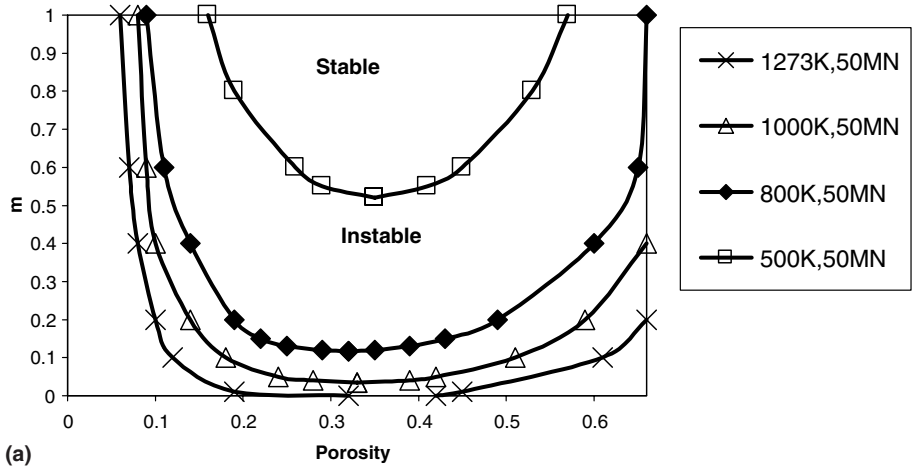


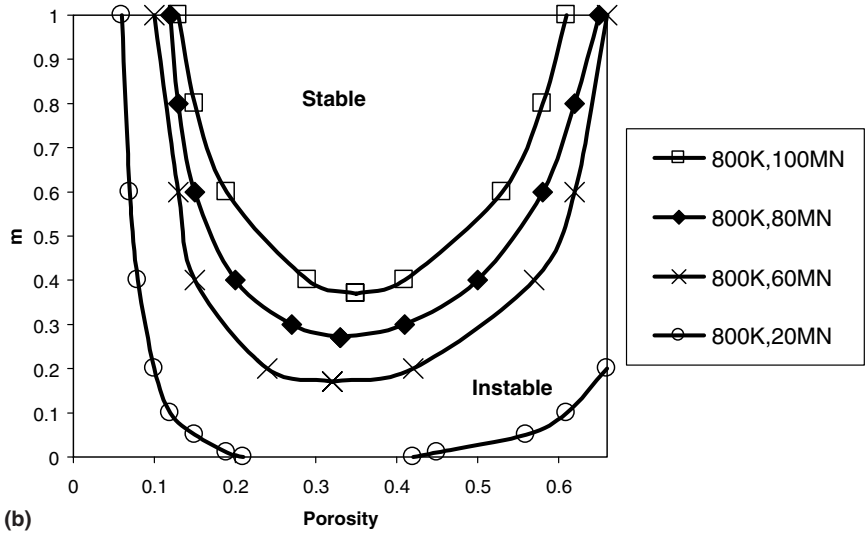


Fig. 2. Stability map for the temperature-coupled non-uniform mode analysis (Skorohod model) of the forging of a copper powder. The activation energy $Q_c = 197$ KJ/mol, heat capacity $c_0 = 384.16$ J/K kg: (a) The load is assumed to be 50 MN. Higher temperature corresponds to higher stability region. (b) The temperature is assumed to be 800 K. Lower stress corresponds to higher stability region.

$$D_3 = \left[ -A'_{\mathrm{T}}\sigma_z \frac{(\phi\psi' - \psi\phi') - \frac{\sqrt{6}\phi^2}{3|n|} + \phi\psi}{\phi\left(\psi - \frac{\sqrt{6}\phi}{3|n|}\right)} - A'_{\mathrm{T}}\sigma_z \left( \frac{4}{1-\theta} + \frac{\phi\psi' n^2 - \psi\phi' n^2}{\phi\psi n^2 + \phi^2} \right) \right] \left( \frac{\psi}{\phi} n^2 + 1 \right)$$
$$\left( \frac{2}{3}\phi - \frac{\sqrt{6}}{3}|n|\psi \right) \frac{1}{A_{\mathrm{T}}\rho_0 c_0 \left( \frac{\sqrt{6}}{3}\,\mathrm{sgn}(\sigma_z) n + 1 \right)(1-\theta)^5 m\phi} \tag{35}$$

For forging, the instability occurs if $\frac{\dot{\lambda}}{\dot{\theta}} < 0$. Stability maps for various materials can be constructed through the assessment of the corresponding values of the coefficients $D_1$, $D_2$, and $D_3$ that can provide only positive roots of Eq. (34). A numerical solution of this problem in terms of porosity and creep exponent $m$ has been carried out for a copper powder. The activation energy was assumed to be $Q_c = 197$ KJ/mol, heat capacity is assumed to be $c_0 = 384.16$ J/K kg (see Ashby, 1990). The threshold value $\left|\frac{\dot{\lambda}}{\dot{\theta}}\right| = 40$ is adopted in the computation since only large enough perturbations will lead to loss of stability eventually according to physical meaning. For the Skorohod model, the results are given in Fig. 2. Fig. 2a shows the stability and the instability areas for constant axial force equal to 50 MN under various temperatures. The results indicate that the growth of the stability area when the temperature increases. Fig. 2b represents the stability and the instability areas for the temperature of 800 K under various axial forces. It can be drawn from the calculation that lower axial force favors stability.

## 4. Conclusions

The temperature-coupled stability analysis indicates that as temperature increases, the stability tendency increases; as pressure decreases, stability region increases. Through the obtained stability maps, the ranges of pressure and temperature, which ensure the stability of forging of porous bodies, can be determined.


## Acknowledgements

This work has been supported by the NSF Division of Manufacturing and Industrial Innovation and NSF International Division, Grants DMI-9985427 and CMS-0301115. The support of A.M. by DGA-France, Grant 02 60 00 064, is gratefully acknowledged.


## References


Ashby, M.F., 1990. Background Reading, HIP 6.0. University of Cambridge, Cambridge, UK.

Lee, J.H., Zhang, Y., 1994. A finite-element work-hardening plasticity model of the uniaxial compression and subsequent failure of porous cylinders including effects of void nucleation and growth. 1. Plastic flow and damage. J. Eng. Mater. Tech.-Trans. ASME 116 (1), 69–79.

Lee, J.H., Zhang, Y., 1996. A finite-element work-hardening plasticity model of the uniaxial compression and subsequent failure of porous cylinders including effects of void nucleation and growth. 2. Localization and fracture criteria. J. Eng. Mater. Tech.-Trans. ASME 118 (2), 169–178.

Olevsky, E.A., 1998. Theory of sintering: from discrete to continuum Invited Review. Mater. Sci. Eng. R. Reviews 23, 41–100.

Olevsky, E.A., German, R.M., 2000a. Effect of gravity on dimensional change during sintering, I. Shrinkage anisotropy. Acta Mater. 48, 1153–1166.

Olevsky, E.A., German, R.M., 2000b. Effect of gravity on dimensional change during sintering, II. Shape distortion. Acta Mater. 48, 1167–1180.

Olevsky, E.A., Molinari, A., 2000. Instability of sintering of porous bodies. Int. J. Plast. 16, 1–37.
Olevsky, E.A., Dudek, H.J., Kaysser, W.A., 1996. HIPing conditions for processing of metal matrix composites using continuum theory for sintering. Acta Metall. Mater. 44, 707–724.
Olevsky, E.A., Skorohod, V., Petzow, G., 1997. Densification by sintering incorporating phase transformations. Scripta Mater. 37, 635–643.
Wilkinson, D.S., Ashby, M.F., 1975. Pressure sintering by power law creep. Acta Metall. 23, 1277–1285.